ELASTODYNAMIC NEAR-TIP FIELDS FOR A CRACK PROPAGATING ALONG THE INTERFACE OF TWO ORTHOTROPIC SOLIDS†

J. D. ACHENBACH, Z. P. BAŽANT and R. P. KHETAN

Department of Civil Engineering, Northwestern University, Evanston, IL 60201, U.S.A.

Abstract—The elastodynamic stress field near a crack tip rapidly propagating along the interface between two dissimilar orthotropic elastic solids is solved numerically, for in-plane motion. The cartesian displacements are sought in the separated forms, $r^p U(\theta)$ and $r^p V(\theta)$, r and θ being polar coordinates centered at the moving tip. This reduces the mathematical statement of the problem to two complex second-order linear ordinary differential equations for complex functions $U(\theta)$ and $V(\theta)$. By means of the finite difference method, a matrix eigenvalue problem of the type $\Sigma A_{ij}(p)X_j = 0$, is obtained where $A_{ij}(p)$ are polynomials of the complex variable p and X_j are complex unknowns. An iterative numerical scheme for determining $Im(p)$ is developed and the roots p as well as angular stress and displacement distributions are calculated and plotted for various material combinations. Comparison with exact solutions for the case of dissimilar isotropic solids indicates good accuracy of the numerical solution. The orthotropic nature of the materials is shown to have a significant effect on stress maximums.

1. INTRODUCTION

IN A PRECEDING paper[1], we investigated the variation with polar angle of the near-tip elastodynamic fields for a crack propagating along the interface between two isotropic elastic solids of different mechanical properties. The nature of singularities near the tips of an interface crack was examined by using an extension to elastodynamic problems of the technique employed by Williams in Ref.[2]. An analogous study for a propagating crack tip in a homogeneous material was presented in Ref.[3]. It was shown in [1] that in the immediate vicinity of the propagating crack tip the stresses show violent oscillations. The radius over which these oscillations are significant depends on the applied loads, and on the speed of the crack tip. The results indicated the magnitudes of stress intensity factors for an arbitrary angle θ, relative to the corresponding factors in the interface.

For a propagating flaw at the interface of two isotropic half-spaces of different mechanical properties, the dependence on polar angle θ of the near-tip stress fields could be determined analytically in explicit form, as shown in Ref[1]. For a flaw at the interface of two anisotropic half-spaces a numerial procedure is required, which is presented in the present paper.

A two-dimensional geometry will be considered. The velocity of the crack tip along the interface is $c(t)$, where $c(t)$ is an arbitrary function of time, subject to the conditions that $c(t)$ and dc/dt are continuous. A system of moving Cartesian coordinates (x, y) is centered at the crack tip, such that the x-axis is in the interface. Moving polar coordinates (r, θ) are attached to the moving crack tip.

2. DISPLACEMENT FORMULATION FOR ORTHOTROPIC MATERIALS

Near-tip stress fields for in-plane motions accompanying the propagation of a crack along the interface between two orthotropic elastic solids are considered. The axes of orthotropy of both solids are assumed to be parallel to the interface $y = 0$. The stress-strain relations for the orthotropic elastic solids may be written in the forms

$$(\tau_x)_j = (E_{xx})_j \frac{\partial u_j}{\partial x} + (E_{xy})_j \frac{\partial v_j}{\partial y}; \tag{1}$$

$$(\tau_y)_j = (E_{yx})_j \frac{\partial u_j}{\partial x} + (E_{yy})_j \frac{\partial v_j}{\partial y}, \tag{2}$$

$$(\tau_{xy})_j = (G_{xy})_j \left(\frac{\partial u_j}{\partial y} + \frac{\partial v_j}{\partial x} \right) \tag{3}$$

in which $(G_{xy})_j$, $(E_{xx})_j$, $(E_{yy})_j$ and $(E_{xy})_j = (E_{yx})_j$ are independent elastic moduli of the two solids

$(j = 1, 2)$. For the special case of isotropic solids we have $(G_{xy})_j = \mu_j$; $(E_{xx})_j = (E_{yy})_j = 2\mu_j(1 - \nu_j)/(1 - 2\nu_j)$; $(E_{xy})_j = (E_{yx})_j = 2\mu_j\nu_j/(1 - 2\nu_j)$.

If eqns (1)–(3) are substituted into the stress equations of equilibrium relative to the coordinate system moving with velocity $c(t)$, and material time derivatives are expanded according to

$$\ddot{u}_j = \frac{\partial^2 u_j}{\partial t^2} - \dot{c}(t)\frac{\partial u_j}{\partial x} - 2c(t)\frac{\partial^2 u_j}{\partial t \partial x} + [c(t)]^2\frac{\partial^2 u_j}{\partial x^2}, \tag{4}$$

two partial differential equations for $u_j(x, t)$ and $v_j(x, t)$ ensue. These equations are analogous to eqns (33) and (34) of Ref. [3]. Similarly to Ref. [3], the cartesian displacement components near the crack tip may be sought in the forms

$$u_j = d\left(\frac{r}{d}\right)^p U_j(\theta)T(t); \quad v_j = d\left(\frac{r}{d}\right)^p V_j(\theta)T(t) \tag{5a, b}$$

where d is a length parameter and U_j and V_j are functions of θ. If the derivatives in the differential equations for u_j and v_j are converted to polar coordinates, expressions (5a, b) are substituted and the limit $r \to 0$ is considered, one obtains the following two ordinary differential equations for U_j and V_j

$$[\{(E_{xx})_j - \beta_j^2(G_{xy})_j\} \sin^2 \theta + (G_{xy})_j \cos^2 \theta]\frac{d^2 U_j}{d\theta^2}$$

$$+ \{(E_{xx})_j - \beta_j^2(G_{xy})_j - (G_{xy})_j\}(1 - p)\sin 2\theta\frac{dU_j}{d\theta}$$

$$+ p\left[\{(G_{xy})_j - (1 - p)[(E_{xx})_j - \beta_j^2(G_{xy})_j]\} \cos^2 \theta\right.$$

$$+ \{(E_{xx})_j - (\beta_j^2 + 1 - p)(G_{xy})_j\} \sin^2 \theta\bigg]U_j$$

$$- \{(E_{xy})_j + (G_{xy})_j\}\left\{\frac{\sin 2\theta}{2}\frac{d^2 V_j}{d\theta^2} + (1 - p)\cos 2\theta\frac{dV_j}{d\theta}\right.$$

$$+ p(2 - p)\frac{\sin 2\theta}{2}V_j\bigg\} = 0 \tag{6}$$

$$\{(1 - \beta_j^2)(G_{xy})_j \sin^2 \theta + (E_{yy})_j \cos^2 \theta\}\frac{d^2 V_j}{d\theta^2}$$

$$+ \{(1 - \beta_j^2)(G_{xy})_j - (E_{yy})_j\}(1 - p)\sin 2\theta\frac{dV_j}{d\theta}$$

$$+ p[\{(E_{yy})_j - (1 - p)(1 - \beta_j^2)(G_{xy})_j\} \cos^2 \theta$$

$$+ \{(1 - \beta_j^2)(G_{xy})_j - (1 - p)(E_{yy})_j\} \sin^2 \theta]V_j$$

$$- \{(E_{xy})_j + (G_{xy})_j\}\left\{\frac{\sin 2\theta}{2}\frac{d^2 U_j}{d\theta^2} + (1 - p)\cos 2\theta\frac{dU_j}{d\theta}\right.$$

$$+ p(2 - p)\frac{\sin 2\theta}{2}U_j\bigg\} = 0. \tag{7}$$

These equations are identical to eqns (36) and (37) of Ref. [3] except for subscript j and p instead of q. Conditions $(\tau_y)_j = 0$ and $(\tau_{xy})_j = 0$ on the surfaces of the crack provide:
    At $\theta = \pm\pi$:

$$\frac{dU_j}{d\theta} = -pV_j,$$

$$(E_{yy})_j\frac{dV_j}{d\theta} = -(E_{xy})_j pU_j \tag{8a, b}$$

For perfect contact the interface conditions are $(\tau_y)_1 = (\tau_y)_2$ and $(\tau_{xy})_1 = (\tau_{xy})_2$, which yield:
At $\theta = 0$:

$$(E_{xy})_1 p U_1 + (E_{yy})_1 \frac{dV_1}{d\theta} = (E_{xy})_2 p U_2 + (E_{yy})_2 \frac{dV_2}{d\theta}$$

$$(G_{xy})_1 \left(\frac{dU_1}{d\theta} + p V_1\right) = (G_{xy})_2 \left(\frac{dV_2}{d\theta} + p V_2\right) \tag{9a, b}$$

$$U_1 = U_2, \quad V_1 = V_2. \tag{10a, b}$$

The stresses may be obtained from eqns (1)–(3) as

$$(\tau_x)_i = d^2 \left(\frac{r}{d}\right)^{p-1} T(t)[T_x(\theta)]_i \tag{11}$$

$$(\tau_y)_i = d^2 \left(\frac{r}{d}\right)^{p-1} T(t)[T_y(\theta)]_i \tag{12}$$

$$(\tau_{xy})_i = d^2 \left(\frac{r}{d}\right)^{p-1} T(t)[T_{xy}(\theta)]_i, \tag{13}$$

where

$$[T_x(\theta)]_i = (E_{xx})_i \left\{p \cos\theta \, U_i - \sin\theta \frac{dU_i}{d\theta}\right\} + (E_{xy})_i \left\{p \sin\theta \, V_i + \cos\theta \frac{dV_i}{d\theta}\right\} \tag{11a}$$

$$[T_y(\theta)]_i = (E_{yx})_i \left\{p \cos\theta \, U_i - \sin\theta \frac{dU_i}{d\theta}\right\} + (E_{yy})_i \left\{p \sin\theta \, V_i + \cos\theta \frac{dV_i}{d\theta}\right\} \tag{12a}$$

and

$$[T_{xy}(\theta)]_i = (G_{xy})_i \left[\left\{p \sin\theta \, U_i + \cos\theta \frac{dU_i}{d\theta}\right\} + \left\{p \cos\theta \, V_i - \sin\theta \frac{dV_i}{d\theta}\right\}\right] \tag{13a}$$

Since p is generally complex, the physical stresses are given by the real parts of eqns (11)–(13). In the following sections numerical results will be obtained for $[T_x(\theta)]_i$, $[T_y(\theta)]_i$ and $[T_{xy}(\theta)]_i$ only. We refer to Ref. [1] for the effect of the multiplying term $d^2(r/D)^{p-1} T(t)$ on the stresses.

3. NUMERICAL SOLUTION

Differential equations (6) and (7), with boundary conditions (8a, b) and with interface conditions (9a, b) and (10a, b), define an eigenvalue problem for p. This problem can be solved by the finite difference method. For this purpose the interval $\theta \epsilon (-\pi, \pi)$ is subdivided into $2n$ equal subintervals $\Delta\theta$ (Fig. 1). To formulate the boundary conditions, one exterior node is introduced near each crack surface. To formulate the interface condition two nodes are introduced at the interface ($\theta = 0$), one for each solid, and in addition one exterior node for each solid is introduced near the interface $\theta = 0$ (see Fig. 1). This gives a total of $m = 2n + 6$ nodes (numbered as $k = 1$, $2 \ldots m$). Each node is associated with two unknowns, namely, the discrete values U_{jk} and V_{jk} of the continuous functions $U_j(\theta)$ and $V_j(\theta)$. The differential eqns (6) and (7) are written for the nodal values $\theta_k (k = 1, 2, \ldots m)$, by approximating the derivatives by finite difference equations. Symmetric fifth-order finite difference expressions of the forms (see Ref.[4], p. 539):

$$\left(\frac{dY}{d\theta}\right)_k \approx \frac{1}{12\Delta\theta}\left(Y_{k-2} - 8Y_{k-1} + 8Y_{k+1} - Y_{k+2}\right) \tag{14}$$

$$\left(\frac{d^2Y}{d\theta^2}\right)_k \approx \frac{1}{12(\Delta\theta)^2}\left(-Y_{k-2} + 16Y_{k-1} - 30Y_k + 16Y_{k+1} - Y_{k+2}\right) \tag{15}$$

with error $O(\Delta\theta)^6$ were used for all nodes which are located more than $2\Delta\theta$ away from both the
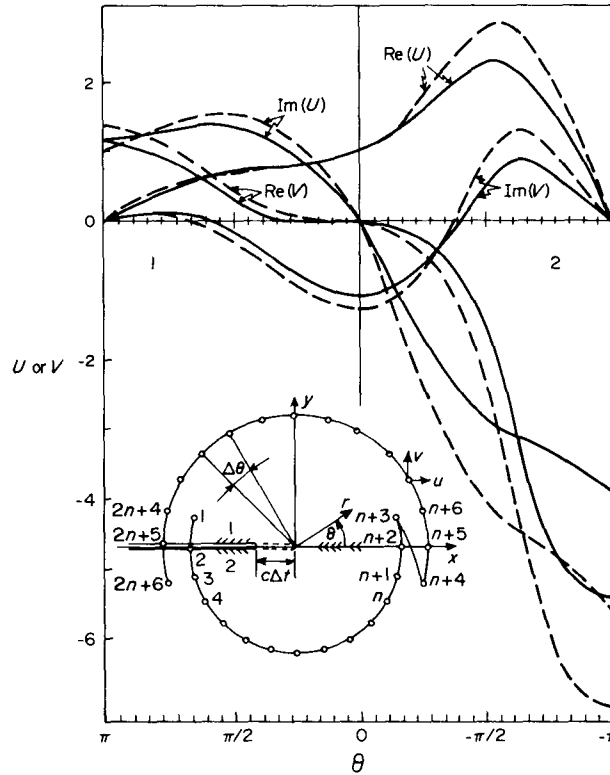
Fig. 1. Angular variation of near-tip displacements. *Case* 1: Analytical results, ——; for isotropic halfspaces with $\mu_1/\mu_2 = 2$, $\rho_1/\rho_2 = 1$, $\nu_1 = \nu_2 = 0.3$, $c^2/c_{R1}^2 = 0.4$, $Im\ p = 0.1432$. *Case* 2: Numerical results, -----; for $\mu_1/\mu_2 = 2$, $\rho_1/\rho_2 = 1$, $\nu_1 = \nu_2 = 0.3$, but $(E_{xx})_1$ doubled as compared to case 1 (i.e., orthotropic halfspace 1), $c^2/c_{R1}^2 = 0.4$, $Im\ p = 0.1633$ and $\Delta\theta = \pi/18$.

crack surface and the interface. (Y represents either U_j or V_j.) For nodes located closer, the usual, third-order symmetric finite difference expressions (see eqns 42 in [3]) were used, in order to avoid the introduction of further exterior nodes at distances $2\Delta\theta$ away from the crack surfaces and the interface. For the same reason, third-order symmetric finite difference formulas were also used in approximating the derivatives in the boundary and interface conditions. The assemblage of the matrix of the finite difference equations was programmed in the same manner as has been described in [3] (except that eqns (44) and (45) from [3] now assume a complex form).

The finite difference equations form a system of $2m$ homogeneous algebraic equations for $2m$ unknowns,

$$\sum_{s=1}^{2m} A_{rs}(p)X_s = 0 \qquad (r = 1, \ldots 2m) \tag{16}$$

in which $X_{2k-1} = U_k$, $X_{2k} = V_k$. Matrix A_{rs} is banded of bandwidth 15, and it is non-symmetric. Because p is, in general, complex, matrix A_{rs} is also complex and the unknown vector X_s must be considered complex. Equation (16) represents a non-standard matrix eigenvalue problem for p, where p appears non-linearly in coefficients A_{rs}.

The coefficients of eqns (6), (7), (8a, b) and (9a, b) are all polynomials in p. Then, in view of eqns (14) and (15), all coefficients of matrix $A_{rs}(p)$ must also be polynomials in p. Noting that the conjugate of a power of a complex number equals the same power of the conjugate number and that the conjugate of a sum or product equals a sum or product of conjugates, the conjugate of eqn (16) may be written as

$$\sum_{s=1}^{2m} A_{rs}(\bar{p})\bar{X}_s = 0 \qquad (r = 1, 2, \ldots 2m) \tag{17}$$

where a superimposed bar denotes a conjugate. From this equation it follows that if $p = p_1 + ip_2$
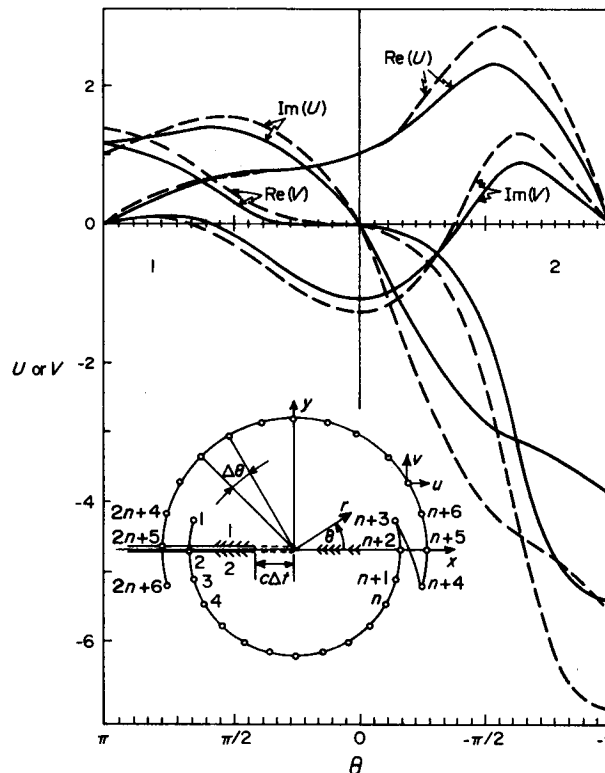
Fig. 1. Angular variation of near-tip displacements. *Case* 1: Analytical results, ———; for isotropic halfspaces with $\mu_1/\mu_2 = 2$, $\rho_1/\rho_2 = 1$, $\nu_1 = \nu_2 = 0.3$, $c^2/c_{R1}^2 = 0.4$, $Im\ p = 0.1432$. *Case* 2: Numerical results, -----; for $\mu_1/\mu_2 = 2$, $\rho_1/\rho_2 = 1$, $\nu_1 = \nu_2 = 0.3$, but $(E_{xx})_1$ doubled as compared to case 1 (i.e., orthotropic halfspace 1), $c^2/c_{R1}^2 = 0.4$, $Im\ p = 0.1633$ and $\Delta\theta = \pi/18$.

crack surface and the interface. (Y represents either U_j or V_j.) For nodes located closer, the usual, third-order symmetric finite difference expressions (see eqns 42 in [3]) were used, in order to avoid the introduction of further exterior nodes at distances $2\Delta\theta$ away from the crack surfaces and the interface. For the same reason, third-order symmetric finite difference formulas were also used in approximating the derivatives in the boundary and interface conditions. The assemblage of the matrix of the finite difference equations was programmed in the same manner as has been described in [3] (except that eqns (44) and (45) from [3] now assume a complex form).

The finite difference equations form a system of $2m$ homogeneous algebraic equations for $2m$ unknowns,

$$\sum_{s=1}^{2m} A_{rs}(p)X_s = 0 \qquad (r = 1, \ldots 2m) \tag{16}$$

in which $X_{2k-1} = U_k$, $X_{2k} = V_k$. Matrix A_{rs} is banded of bandwidth 15, and it is non-symmetric. Because p is, in general, complex, matrix A_{rs} is also complex and the unknown vector X_s must be considered complex. Equation (16) represents a non-standard matrix eigenvalue problem for p, where p appears non-linearly in coefficients A_{rs}.

The coefficients of eqns (6), (7), (8a, b) and (9a, b) are all polynomials in p. Then, in view of eqns (14) and (15), all coefficients of matrix $A_{rs}(p)$ must also be polynomials in p. Noting that the conjugate of a power of a complex number equals the same power of the conjugate number and that the conjugate of a sum or product equals a sum or product of conjugates, the conjugate of eqn (16) may be written as

$$\sum_{s=1}^{2m} A_{rs}(\bar{p})\bar{X}_s = 0 \qquad (r = 1, 2, \ldots 2m) \tag{17}$$

where a superimposed bar denotes a conjugate. From this equation it follows that if $p = p_1 + ip_2$

is a root, then $\bar{p} = p_1 - ip_2$ is also a root, and if eigenvector X_r is associated with root p then the eigenvector associated with $\bar{p}$ is $\bar{X}_r$ or $C\bar{X}_r$, where C is any non-zero complex number.

The numerical solution is facilitated by the fact that $Re(p)$ must equal 0.5. The proof can be based on energy balance conditions, considering the flux $\mathscr{E}$ of energy into a small circular region (of radius r) which encircles the tip of the propagating crack and moves with it.

In the special case of two identical solids, $p = 0.5$ is known to be a double root. Therefore, the two conjugate complex roots p and $\bar{p}$ for the case of two dissimilar solids must be simple roots. Consequently, only one eigenvector must be associated with each of the roots p and $\bar{p}$. In the special case of $p = 0.5$ (real), there are two linearly independent eigenvectors associated with p; they may be chosen to represent the Modes I and II, and all of their (infinitely numerous) linear combinations also represent eigenvectors. From this consideration it is clear that the ratio σ_θ/σ_r or $U_{\theta 0}/U_{r0}$ (where $\sigma_\theta = [T_y(0)]_j$, $\sigma_{\theta r} = [T_{xy}(0)]_j$, $U_{\theta 0} = [V(0)]_j$ are $U_{r0} = [U(0)]_j$ are the interface values) must have a certain (complex) value when $Im(p) \neq 0$, while any value is possible when $p = 0.5$ (real). This conclusion agrees with the fact that according to eqn (60) (or eqn (61)) of Ref.[1] for two isotropic materials the ratio $\sigma_\theta/\sigma_{\theta r}$ (or $U_{\theta 0}/U_{r0}$) is fixed. It is also clear that, in order to uniquely specify an eigenvector for $Im(p) \neq 0$, only one among the (complex) values $X_r(r = 1, \ldots 2m)$ may be chosen (the amplitude). On the other hand, when $p = 0.5$ (real), two values among the (real) values X_r must be chosen in order to specify the eigenvector uniquely.

One interesting property of the solution for two dissimilar isotropic solids is that the ratio $\sigma_{\theta r}/\sigma_\theta$ of interface stresses and $U|_{\omega}/U_{r0}$ of interface displacements is purely imaginary (eqns (60) and (61) of Ref.[1]). The limited numerical results obtained indicate that this is also true for dissimilar orthropic solids. When the case of two identical solids is approached $(Im(p) \rightarrow 0)$, $\lim(\sigma_{\theta r}/\sigma_\theta)$ at $\theta = 0$ is also purely imaginary $(= ik)$ and the eigenvector associated with root p tends to $X_r^A = X_r^I + ikX_r^{II}$ where X_r^I and X_r^{II} are the eigenvectors for Modes I and II, while the eigenvector associated with root $\bar{p}$ tends to $X_r^B = X_r^I - ikX_r^{II}$. Thus, Modes I and II cannot be obtained directly as the limit of X_r but they appear as linear combinations of complex eigenvectors X_r^A and X_r^B.

The root, p, and the corresponding eigenvector, X_r, may be computed by the following procedure which is similar to the one developed in Ref. [5] and employed in Ref. [3]. First the matrix $A_{ij}(p)$ is evaluated for a chosen value of $p = p_1 + ip_2$. Then the equation for one of the unknowns X_r, e.g., for the $X_k = V_{jk}$ at the interface node $n + 2$ ($k = 2n + 3$), is deleted from the matrix A_{rs} (and is stored separately). This equation is then replaced by the equation $X_k = 1$ (real), which makes the equation system nonhomogeneous. Its matrix becomes non-singular because p is a simple root when $Im(p) \neq 0$. Hence, it is possible to solve the system of equations, whereby standard library routines for complex matrices may be used. (If it is necessary to keep the cost of computation low, a special equation solver for banded complex matrices is needed; but the necessary size of the matrix can be handled with regular square matrix subroutines.) After solving the unknowns X_r, the right-hand side Z_k of the original k^{-th} equation is evaluated. The quantity Z_k may be regarded as a function of $Im(p)$ or p_2, which is chosen at the beginning of the procedure, i.e., $Z_k = Z_k(p_2)$. Subsequently, the whole solution is repeated for other chosen values of p_2 and the iterative "regula falsi" method is utilized to find the value of p_2 which yields $Z_k = 0$ (i.e., $Re(Z_k) = Im(Z_k) = 0$). The solution for this case represents the displacement eigenvectors U_{jk} and V_{jk} and the corresponding stresses may be evaluated using finite difference formulas. Note that if $Re(p)$ were not known it would have to be varied, too, and the search for the root would then be considerably more time consuming.

Because the finite difference equations represent only an approximate formulation, the real part of the exact eigenvalue p of the discrete problem does not equal exactly 0.5 (e.g., for the case when $\mu_1/\mu_2 = 0.5$, $(c/c_{R1})^2 = 0.4$ and $n = 18$, $Re(p) = 0.5006$). It seems, however, more appropriate as well as more convenient to keep $Re(p)$ exactly equal 0.5. As a consequence of this choice $Re(Z_k)$ and $Im(Z_k)$ do not become zero for exactly the same value of p_2. The objective in the iterative "regula falsi" has, therefore, actually been considered achieved when $Im(Z_k) = 0$, instead of $Im(Z_k) = Re(Z_k) = 0$. The value of $Re(Z_k)$ associated with $Im(Z_k) = 0$ was very small but non-zero; see Fig. 6b. The condition $Im(Z_k) = 0$ gave more accurate results than the condition $Re(Z_k) = 0$ because $Im(Z_k)$ exhibited always a steeper variation. The difference between the values of p_2 which made $Im(Z_k) = 0$ and $Re(Z_k) = 0$ was very small and diminished with $\Delta\theta$. Another consequence of the fact that $Re(p)$ is not exactly 0.5 for the discrete problem, is that the

eigenvector obtained for $\bar{p}$ is close but not exactly equal to the conjugate of the eigenvector obtained for p (times a complex constant).

When the root p is real, it is a double root and two linearly independent eigenvectors are associated with it. Then it is necessary to prescribe two of the values X_r; e.g. $X_k = 1$ and $X_{k+1} = 0$. If only one value were prescribed the equation system would remain singular. When p is complex but $Im(p)$ is very small, still one value ($X_k = 1$) can be prescribed but because of the proximity to the case of a double root, the equation system is close to a singular matrix and it is, therefore, ill-conditioned. The numerical procedure described previously then breaks down. However, the case of very small $Im(p)$ is of little practical concern.
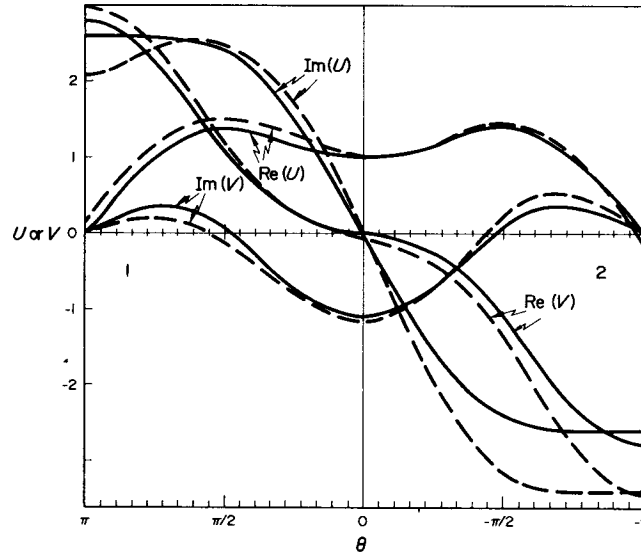

Fig. 2. Angular variation of near-tip displacements. *Case* 1: Analytical results, ———; for identical isotropic halfspaces with $\nu_1 = \nu_2 = 0.3$, $c^2/c^2_{R1} = 0.4$, $Im\ p = 0$ and $Im\ (U$ or $V) = 1.0822$ times Mode II displacement for $U_{\theta o} = 1$. *Case* 2: Numerical results, -----; for $\mu_1/\mu_2 = 1$, $\rho_1/\rho_2 = 1$, $\nu_1 = \nu_2 = 0.3$ but $(E_{xx})_1$ doubled as compared to case 1, $c^2/c^2_{R1} = 0.4$, $Im\ p = 0.0241$ and $\Delta\theta = \pi/18$.
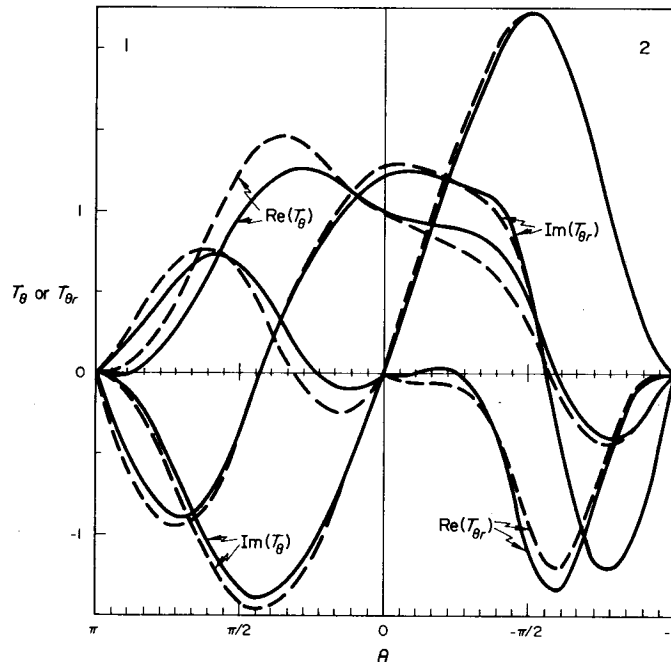

Fig. 3. Angular variation of near-tip stresses: *Case* 1: Analytical results, ———; and *Case* 2: Numerical results, -----; as described in Fig. 1 caption.
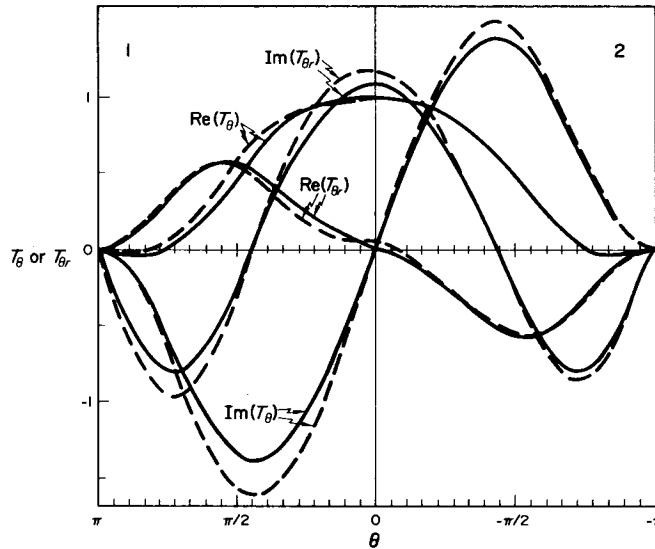
Fig. 4. Angular variation of near-tip stresses: *Case* 1: Analytical results, ——; and *Case* 2: Numerical results, ----; as described in Fig. 2 caption except for Case 1, where $Im(T_\theta$ or $T_{\theta r}) = 1.0822$ times Mode II stress for
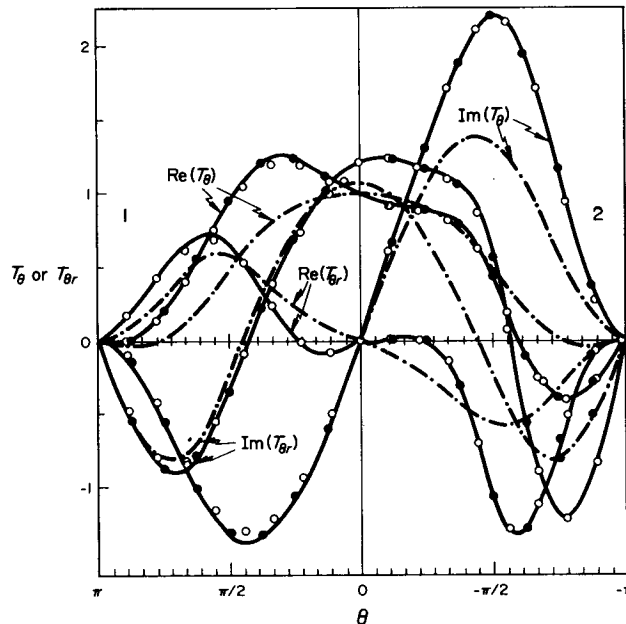
$$\sigma_{\theta r} = 1.$$

Fig. 5. Angular variation of near-tip stresses. *Case* 1: Analytical results, ——; for isotropic halfspaces with $\mu_1/\mu_2 = 2$, $\rho_1/\rho_2 = 1$, $\nu_1 = \nu_2 = 0.3$, $c^2/c_{R1}^2 = 0.4$, $Im\ p = 0.1432$; and corresponding numerical results for $\Delta\theta = \pi/18$ and $\Delta\theta = \pi/32$. *Case* 2: Analytical results, —·—; for identical isotropic halfspaces with $\nu_1 = \nu_2 = 0.3$, $c^2/c_{R1}^2 = 0.4$, $Im\ p = 0$; corresponding numerical results are indistinguishable for both step sizes. $\bigcirc$, $\Delta\theta = \pi/18$; ●, $\Delta\theta = \pi/32$.

4. RESULTS

Numerical results are exhibited in Figs. 1–6. Figure 1 (3) shows a comparison of displacement (stress) distributions for two isotropic halfspaces having different shear moduli and being identical otherwise, with displacements (or stresses) for the case when the halfspace with the lower shear modulus is made orthotropic by doubling its $(E_{xx})_1$ - modulus. Displacement (stress) distributions for two identical halfspaces are compared with the same for the case when one of the halfspaces is made orthotropic by doubling $(E_{xx})_1$ - modulus, in Fig. 2 (4). The results for two isotropic halfspaces are exact and are obtained from analytical results of Ref. [1], while those involving an orthotropic halfspace are approximate numerical results. Figure 5 gives a picture of accuracy for various step sizes $\Delta\theta$. It appears that for the same $\Delta\theta$, the error gets somewhat
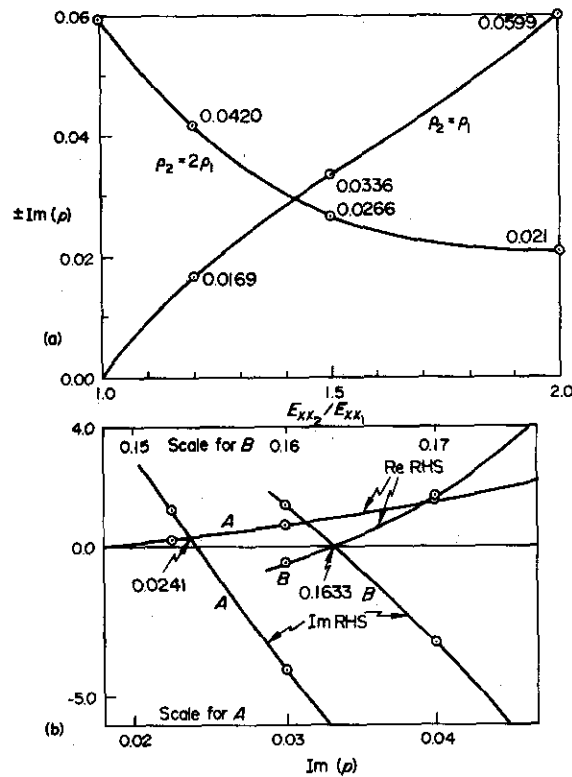
Fig. 6. (a) Dependence of $Im(p)$ on $(E_{xx})_2$ for $\mu_1/\mu_2=1$, $\nu_1=\nu_2=0.3$, $c^2/c_T^2=0.6$, $(E_{xx})_1=2\mu_1(1-\nu_1)/(1-2\nu_1)$, $\Delta\theta=\pi/24$ (i.e. isotropic halfspace 1). (b) Dependence of the right-hand side (RHS) of the k-th equation on Im (p). A: $\mu_2/\mu_1=1$, $\rho_1/\rho_2=1$, $\nu_1=\nu_2=0.3$, $c^2/c_{R2}^2=0.4$, $(E_{xx})_2=2(E_{xx})_1=4\mu_1(1-\nu_1)/(1-2\nu_1)$, $\Delta\theta=\pi/18$. B: $\mu_2/\mu_1=2$, $\rho_1/\rho_2=1$, $\nu_1=\nu_2=0.3$, $c^2/c_{R2}^2=0.4$, $(E_{xx})_2=2(E_{xx})_1=4\mu_1(1-\nu_1)/(1-2\nu_1)$, $\Delta\theta=\pi/18$.

Table 1. Comparison of numerical and analytical results for $Im(p)$, for the case of two joined isotropic half-spaces; $c^2/c_{T2}^2=0.6, \Delta\theta=\pi/24$

ρ_2/ρ_1	μ_1/μ_2	ν_1	ν_2	Im (p)	
				Exact	Numerical
1	1	0.3	0.3	0	0.0003
1	1.2	0.3	0.3	0.0420	0.0428
1	2	0.3	0.3	0.1055	0.1067
2	2	0.3	0.3	0.0590	0.0583
1	1	0.1	0.4	0.1120	0.1112

higher as $|Im(p)|$ grows. The displacement distributions in Figs. 1 and 2 have been normalized to give $U_{r0}=1$ (real), and stress distributions in Figs. 3, 4 and 5 have been normalized to give $\sigma_\theta=1$ (real). To get the displacement distributions associated with $\sigma_\theta=1$, one has to multiply the values shown in Fig. 1 by $(1.4462-0.4141\,i)/\mu_1$ (for isotropic case) or by $(0.971-0.311\,i)/\mu_1$ (for orthotropic case), and those in Fig. 2 by $0.7038/\mu_1($ for isotropic case) or by $(0.557-0.021\,i)/\mu_1$ (for orthotropic case).

Figure 6(a) gives two examples of the dependence of $Im(p)$ upon the degree of orthotropy of one halfspace and Table 1 indicates some numerical results for $Im(p)$ together with the corresponding exact values. Figure 6(b) illustrates the procedure for obtaining $Im(p)$, which was described earlier.

REFERENCES

[1] J. D. ACHENBACH, Z. P. BAŽANT and R. P. KHETAN, Int. J. Engng Sci. 14, 811 (1976).
[2] M. WILLIAMS, Bull. Seism. Soc. Am. 49, 199 (1959).
[3] J. D. ACHENBACH and Z. P. BAŽANT, J. Appl. Mech. 42, 183 (1975).
[4] L. COLLATZ, The Numerical Treatment of Differential Equations, p. 539. Springer-Verlag, Berlin (1960).
[5] Z. P. BAŽANT, I.J. Engng Sci. 12, 221, (1974).